A Statistical Analysis of Brazed Joint Fatigue Behavior

Fatigue life was analyzed and a correlation was made between ultrasonic inspection data and fatigue life distribution

BY H. D. SOLOMON

ABSTRACT. This paper describes the statistical distribution of brazed Cu joints fatigue lives. It describes an approach for setting requirements for braze coverage and the determination of the resulting statistical distribution of the fatigue lives. Such an approach should greatly improve the reliability of brazed structures.

In this study, each joint was inspected ultrasonically and the results of these inspections correlated with the fatigue behavior. Several transducers were used for this ultrasonic measurement. Both the average of all transducer measurements and the single largest measurement were used to set joint quality standards. Limits of 10% were set on the average reflection of all transducers (corresponding to an average incomplete brazing of the joint), and 13% for the maximum reflection of any transducer. Even with these stringent standards, the average projected fatigue life had to be about 10^9 cycles to exceed a 10^4 cycle design life with a high degree of reliability. This observation points up the high degree of scatter in the fatigue behavior of brazed joints and the need to overdesign them so that the fatigue life of the poorest joint will meet the design life.

Introduction

It is well known that brazed joints generally have a lower fatigue life than the metals being joined (Refs. 1, 2). This degradation, relative to the properties of the base and braze metals, stems from defects that develop in the braze. There are three general types of defects: 1) a lack of coverage due to the largely unavoidable small voids that develop during brazing, 2) more gross defects due to larger lack of coverage regions and 3) geometrical discontinuities such as misalignment, undercuts and crowns. Both of the first two types of defects were present in this study. This study did not specifically deal with the third type of defect. Since the actual product joints are not machined after brazing, the tested specimens were also not machined after brazing. This left any small geometrical discontinuities (no large ones were noted) as part of the specimen variation that led to the variation in the fatigue life. Here, the focus was on the degree of coverage and how this influenced the fatigue life. This data was then used to set a coverage specification.

All too often, a structure is designed without properly accounting for the degrading influence of any brazed joints on the design life of that structure. If account is taken of the presence of the brazed joint, it is often insufficient to guarantee a high degree of reliability. This paper shows a statistical approach for determining the fatigue life as a function of braze coverage. It describes the results of a study performed to answer two simple, but critical, questions: What is the statistical variation of the fatigue life, and what is the acceptable ultrasonic reflection level required to statistically meet a required design life? The answer to the first question required a statistical analysis of fatigue behavior, which is described here. The answer to the second question required a correlation of ultrasonic inspection data with the distribution of fatigue lives. This is also described.

The scatter (statistical distribution [Refs. 3–9]) in fatigue data can be significant even when considering carefully machined laboratory fatigue specimens that do not contain joints. The situation is even more complex when joints are present. The defects produced in joints and statistical distribution of these defects further increase the scatter in the fatigue life over that observed in specimens that do not contain a joint. Thus, there generally is a very large distribution in the expected fatigue lives of joints, which must be accounted for when predicting the fatigue behavior. This study describes one way to do this.

Neither the braze process development nor the ultrasonic inspection system was a specific subject of this study. Rather, the quality of the joints, as defined by an ultrasonic inspection, and how this quality impacted the statistical distribution of the fatigue lives were of importance. Some aspects of the statistical evaluation of fatigue data are included as an appendix to this paper.

KEY WORDS

Brazing
Brazed Joint
Fatigue Life
Joint Clearance
Statistical Distribution
Ultrasonic Reflection
Lap Joint

Experimental Procedures

The joints tested in this study were made under the same conditions as actual product joints, by the same individuals, using the same equipment. Proprietary considerations prevent a more complete discussion of the joint process development, but this is not an impediment as we are concerned solely with the statistics of joint quality and the resulting fatigue life.

Two types of joints were made, tested and analyzed. Some specimens, denoted as being large specimens, had a nominal cross section of 1.8 in. wide (45.72 mm) by 0.375 in. thick (9.525 mm). A smaller, medium-sized specimen was also tested. This specimen had a cross section 1.2 in. wide (30.48 mm) by 0.275 in. (6.985 mm) thick. In both cases, the joints were made by induction butt joint brazing two Cu bars together. The joint area was calculated from the nominal area of the joint. All of the joints were ultrasonic

H. D. SOLOMON is with General Electric R&D Center, Schenectady, N.Y.

tested (UT), and the reflections determined at various positions along the joint were ascribed to a lack of brazing (LOB). These measurements were made independently of the fatigue testing program, and, in many cases, the results were not available until the fatigue testing was completed.

The material brazed was C11300 copper (silverbearing, tough pitch Cu, *i.e.*, 99.9 Cu, 0.04 O and the 8 oz/ton Ag; purchased as EMPIS #B11B4, also ASTM B48), brazed with BCuP-5 (Cu with 15 wt-% Ag and 5 wt-% P; purchased as EMPIS B20A6), brazed at 1200–1300°F (650–700°C). The braze thickness ranged from about 50 to 150 microns (2 to 6 mils).

All of the fatigue testing was done on the as-brazed specimens. No machining or surface conditioning was performed after brazing. This enabled the testing of as-brazed joints without modifications to improve the joint quality by removing any braze material that overflowed the joint, or removing any of the Cu to eliminate any undercut of the braze. Thus, the tested braze was exactly the same as the actual product joint, which was also not altered after the brazing operation. Figure 1 shows one of the larger specimens prior to testing.

All testing was done at room temperature in a servo-hydraulic testing machine. The test bars were cut to 6-in. lengths (3 in. on either side of the brazed joint) and held in hydraulic grips,

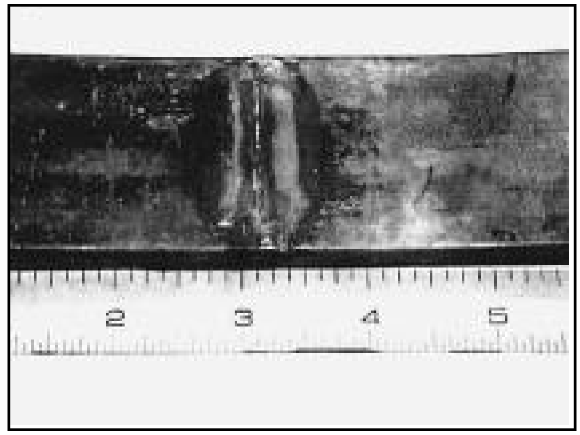

Fig. 1 — Test sample (larger size).

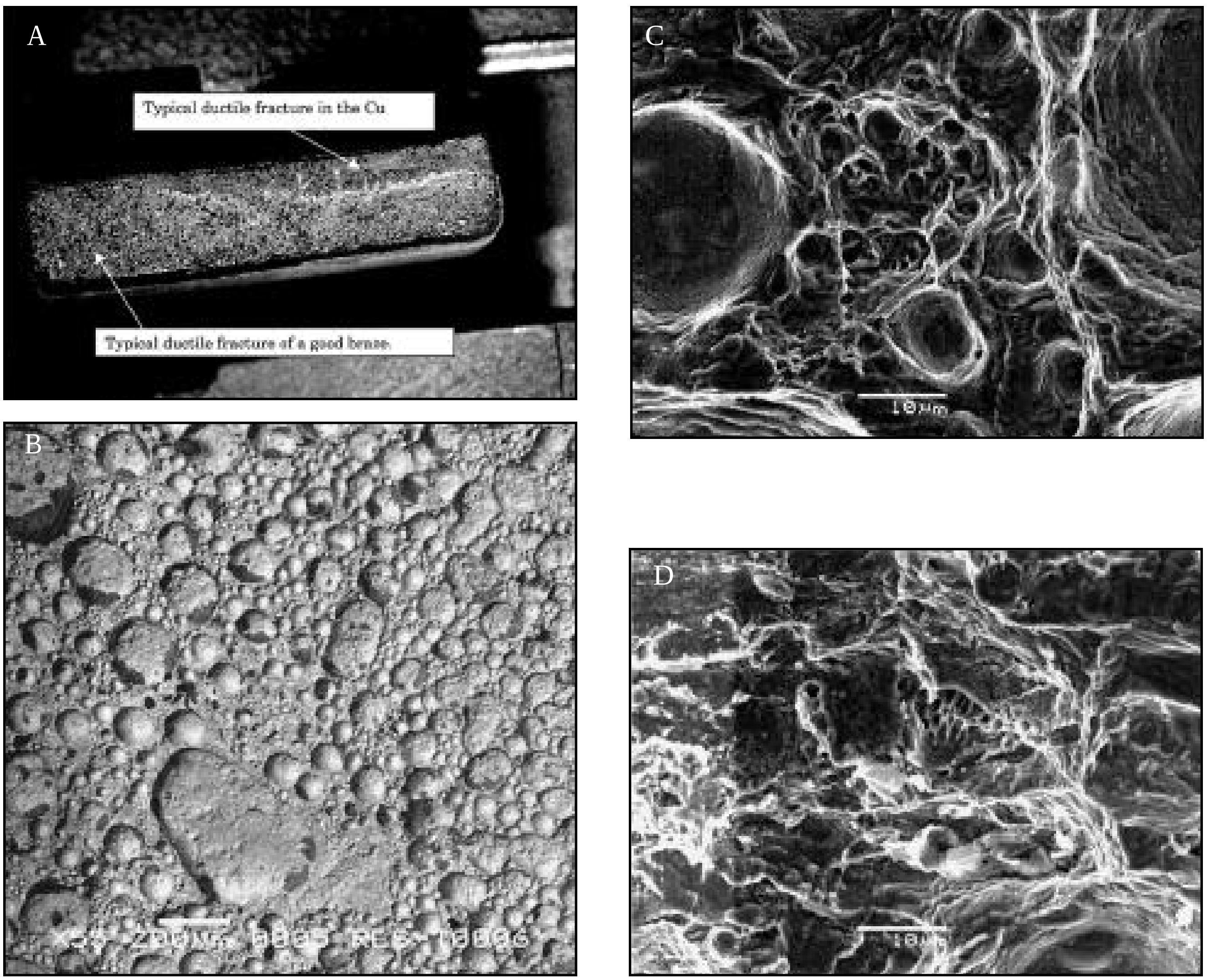

Fig. 2 — Fracture surface for a typical joint. A — Low magnification of the fracture surface; B — higher magnification showing the voids in the braze that were produced during brazing; C — higher magnification showing the voids produced during brazing and those smaller ones (on the ridges between the large voids) produced by the ductile failure of the braze; D — ductile failure in the Cu.

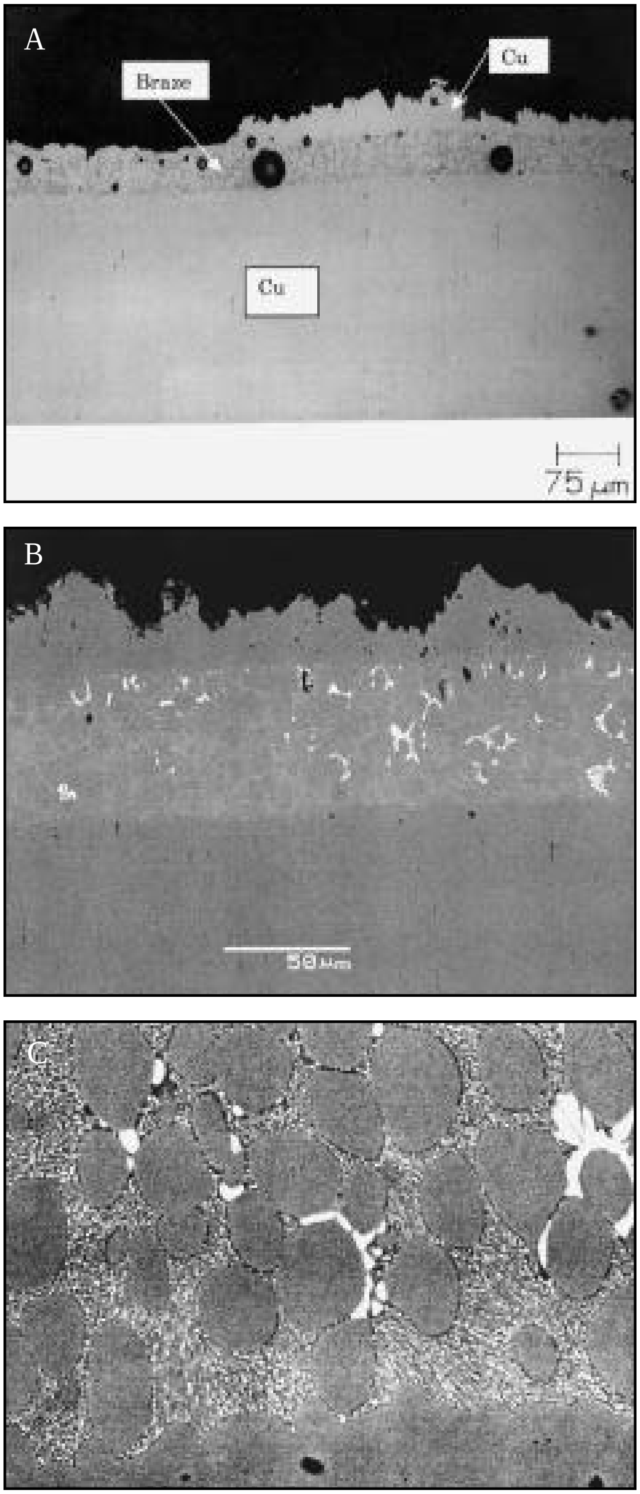

Fig. 3 — Cross section of a typical joint. A — Optical micrograph; B — SEM of the joint cross section. The light regions are Ag-rich; lighter indicates, the more Ag; C — higher magnification of B.

which were locked in place, allowing tensile and compressive loads to be applied. The gripping was on the flat, 1.8-in. (45.72-mm) or 1.2-in. (30.48-mm) faces, with the tensile stress perpendicular to the brazed joint. A simple load-controlled, ramp load/unload cycle was used with 20-Hz cycling frequency. All of the tests described here were performed with fully reversed cycling, *i.e.*, with zero mean stress or R = –1 (where R = min. load/max load, which for fully reversed cycling equals –1 because the minimum load is equal to minus the maximum load).

Results and Discussion

Prior to testing, all brazed samples were subjected to an ultrasonic examination. A multiple transducer array was used to generate and receive an array of ultrasonic signals. This allowed a measurement of joint quality at several points along the joint. Both the magnitudes of the individual transducer measurements as well as the average of all transducer readings were used to assess joint quality. The individual transducer measurements reflect the behavior at individual points along the joint, whereas the average values give an overall picture of the joint. Both measurements were used to assess the quality of the joints. Unfortunately, the ultrasonic inspection technique is proprietary, so more details cannot be given here. Rather, we will focus on how to employ such measurements.

Ultrasonic reflections occurred because the joints were not perfect. Voids developed in all of the brazed joints, an example of which is shown in the fracture surface of Fig. 2. Typical voids, which develop in the brazing process, are shown at a higher magnification in Fig. 2B. These voids contribute to the reflection of the ultrasonic waves. The more the joint area covered by voids, the greater the reflection and the poorer the joint. Very small voids located on the ridges of the larger voids are also visible. It is believed these very small voids, shown in Fig. 2C, result from ductile fatigue failure of the braze.

Much of the fracture surface of Fig. 2 is copper-colored, as opposed to the silver-colored braze. A typical area where the failure was within the Cu is shown in Fig. 2D. The failure also exhibits a typical ductile appearance. The presence of Cu on the fracture surface means the fracture was not entirely within the braze, but went partly through the Cu. This is also shown in Fig. 3, which shows a cross section of a failed joint.

Large voids in the braze are also clearly shown in this figure. Some of these voids extend almost completely through the braze. Figure 3 also shows that some of the failure was through the Cu. In some tests the failure was completely within the Cu, away from the braze. These results were not treated specially in the analysis. This was deemed to be a conservative approach because it would have required a greater number of cycles to cause a failure in the braze. It is believed the Cu failures result from the fact that load-controlled tests were employed. If the strength of the braze is greater than that of the Cu, then, the influence of the defects in the braze not withstanding, the Cu would be the preferred site for failure. That most of the failures were in the braze is testament the defects in the braze generally reduced fatigue life.

Much of the failures in the Cu were traced to the preparation of the surfaces to be brazed. There was some proprietary optimization to improve surfaces to be joined, and all of the joints discussed here were made using this optimized joint preparation.

Figure 4 shows the fracture surface of a specimen that contained large brazed regions (the black-colored regions). There was no braze in these regions, and the machining marks from the base metal prebraze preparation are clearly visible. This is indicative of the region having never been wet with the braze. These regions also show evidence of char due to the decomposition of some organic material that prevented wetting by the braze.

Together, these large unbrazed areas and the smaller voids give rise to the UT reflections that are being ascribed to a lack of braze, LOB. In addition to the voids and unbrazed areas, ultrasonic reflections can also arise from the two-

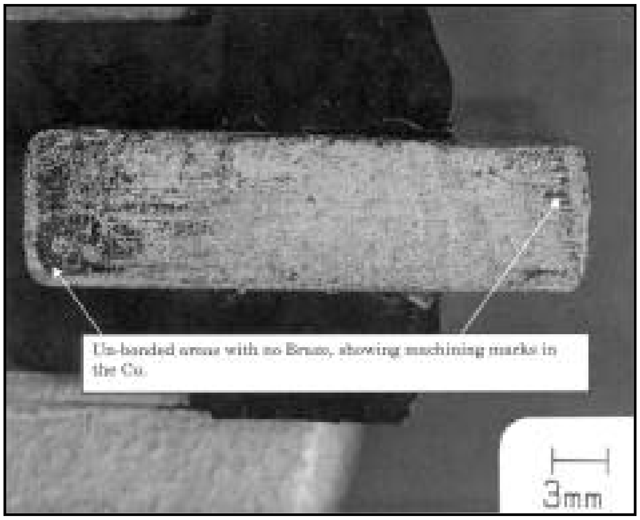

Fig. 4 — Fracture surface of a poorly brazed joint.

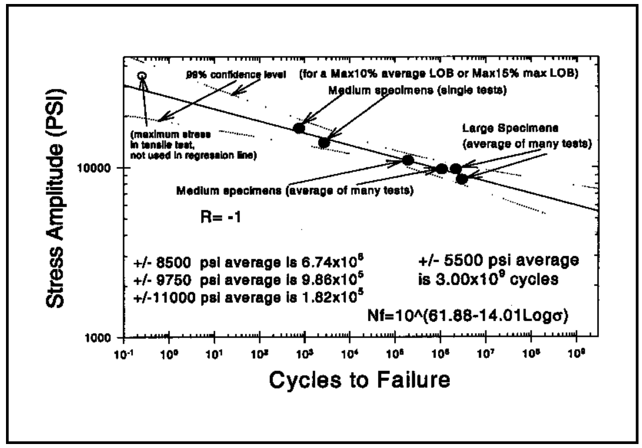

Fig. 5 — S-N curve, R = –1.

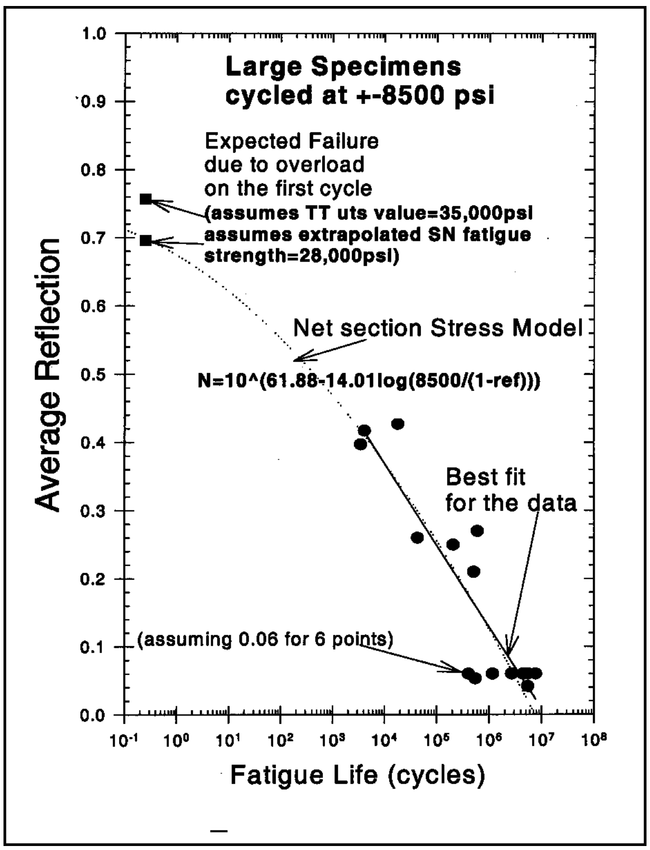

Fig. 6 — Fatigue life vs. the average reflection (LOB) for specimens cycled ±8500 lb/in.^{2} (±59 MPa).

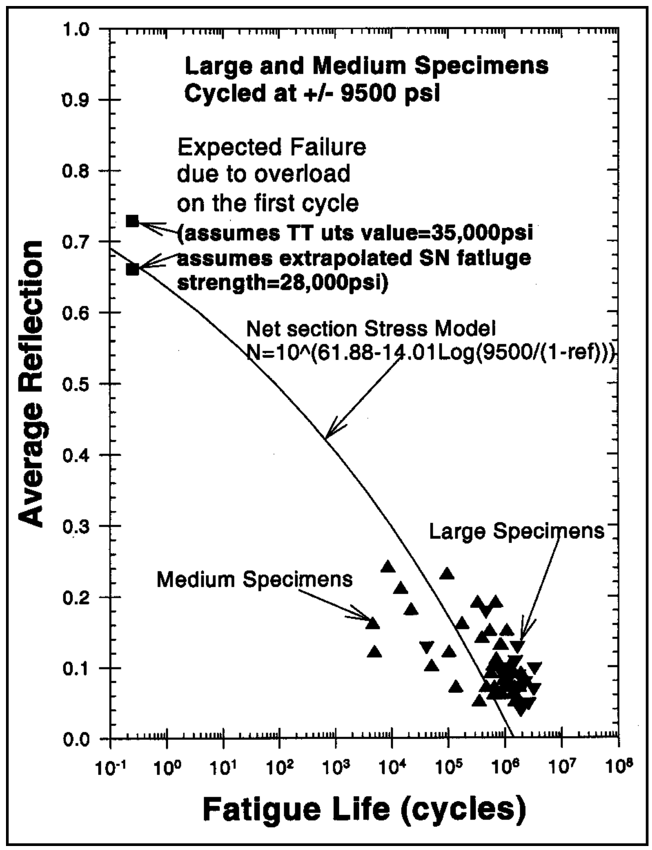

Fig. 7 — Fatigue life vs. the average reflection (LOB) for specimens cycled ±9750 lb/in.^{2} (±67 MPa).

phased nature of the braze, and at the braze/base metal interface (due to elastic property differences). It was beyond the scope of this study to define the source of the reflections in each specimen. Rather, reflection information was used as a metric that a fabricator could employ to define an acceptable braze. This assessment was made based on the correlation of fatigue life distribution with this reflection data.

One of this study's goals was to predict the component life as a function of the ultrasonically measured lack of braze. The service stress was assumed to be ±5500 lb/in.^{2} (±38 MPa). (The actual stresses being applied were more complicated, involving a range of stresses and mean stresses, but this value is appropriate for the analysis being illustrated.) Unfortunately, this small a stress level re-

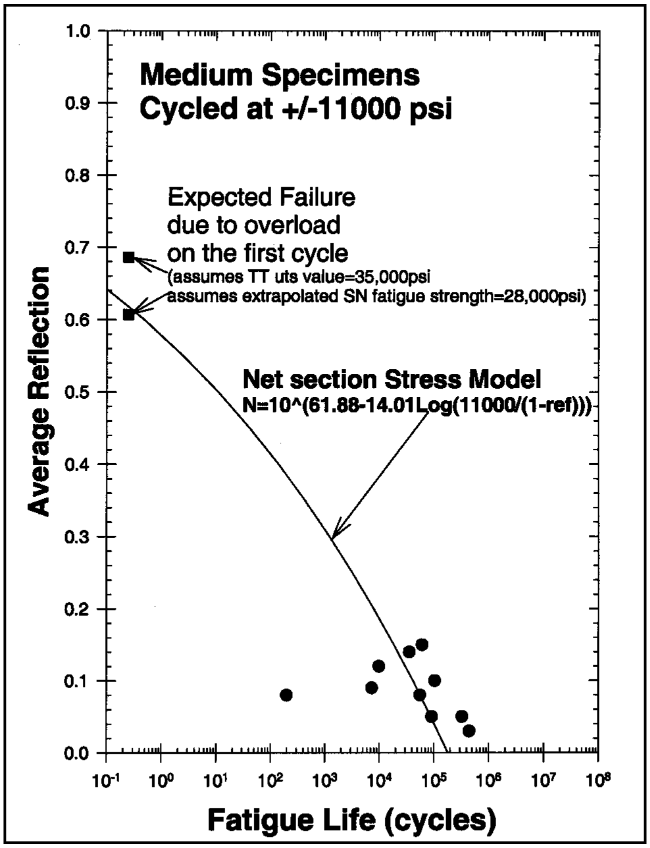

Fig. 8 — Fatigue life vs. the average reflection (LOB) for specimens cycled ±11,000 lb/in.² (±75.5MPa).

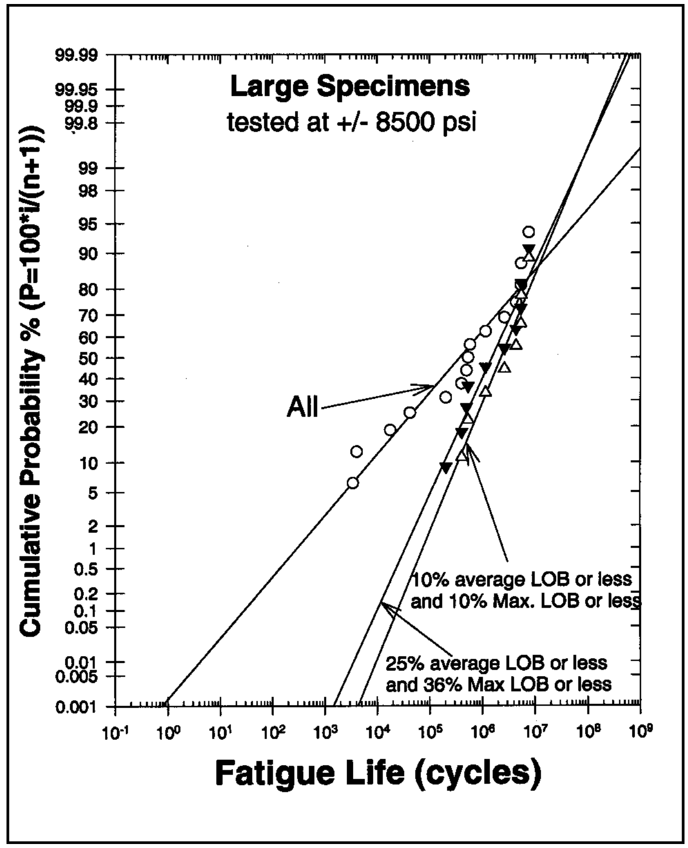

Fig. 9 — Cumulative probability for specimens tested at ±8500 lb/in.² (±59MPa).

sulted in a fatigue life that was too long to allow testing in a reasonable amount of time. It was, therefore, necessary to test at higher stress levels and then to extrapolate this data to the lower stresses of interest. (This extrapolation involves certain inherent assumptions that will be discussed shortly.) Figure 5 shows fatigue life as a function of stress amplitude for fully reversed R = –1 cycling. A series of tests was run at different stress amplitudes, with numerous specimens being run at three of these amplitudes. The data of this figure was obtained with specimens that were deemed to be of highest quality, *i.e.*, the average reflection was ≤10% and no single transducer channel had a reflection (LOB) that was >15%. This data was used to develop a stress-fatigue life plot that was used to extrapolate to the lower stress levels.

The curve fit was developed from the individual data points obtained at ±14000 lb/in.² (±97 MPa) and ±17000 lb/in.² (±112 MPa), and the averages of numerous tests run at lower stress amplitudes. The least squares fit gave the following:

$$N_f = 10\text{^}(61.88-14.01\text{Log}\sigma) \qquad (1)$$

where N_f is the average fatigue life for the applied stress amplitude, σ. This equation was used to extrapolate the data down to ±5500 lb/in.² (±36 MPa). The analysis was also performed without the two highest stress points, where only single tests were run (*i.e.*, the results at ±14,000 lb/in.² and ±17,000 lb/in.²) with no significant change in the life at ±5500 lb/in.².

There is, however, generally some curvature in an S-N curve (Ref. 10), but none was observed here. Furthermore, it was assumed there was no curvature between the lowest stress employed in testing and ±5500 lb/in.². The extrapolation down to ±5500 lb/in.², therefore, produces a conservative approximation, as any curvature in the S-N curve would result in a longer fatigue life than what is predicted when neglecting this effect. The 99% confidence band for the correlation with Equation 1 is shown on the figure. The figure also lists the value of the fatigue lives obtained at different stress amplitudes. As can be seen, cycling at ±5500 lb/in.² (±36 MPa) would yield an average fatigue life of 3 x 10^9 cycles. At 20 Hz it would take more than 41,000 hours (more than 4.5 years) to accumulate this many cycles. Extrapolation was thus the only way to estimate the fatigue life at this stress amplitude. It should be kept in mind, however, the value of 3 x 10^9 cycles is the average fatigue life, but from a reliability standpoint, what is critical is the time for the first failures. Thus, what is critical is the statistics of the failures. This statistical correlation will be considered after the correlation of the reflection data and the fatigue life is discussed.

Figures 6-8 show the average transducer reflection for the joints as a function of the fatigue life. As can be seen, the greater the average reflection (denoting more defects in the joint), the lower the fatigue life. The net section stress model that correlates this data utilizes Equation 1 and the assumption that the average reflection correlates with the load bearing cross section, which equals the nominal cross-sectional area times (1 - average reflection). For instance, in a sample with a 0.25 average reflection, it is assumed the cross-sectional area that can support a load is only (1–0.25) = 0.75 of the nominal cross-sectional area, so the stress is (1/0.75) times the nominal stress. This very simple model appears to do a rea-

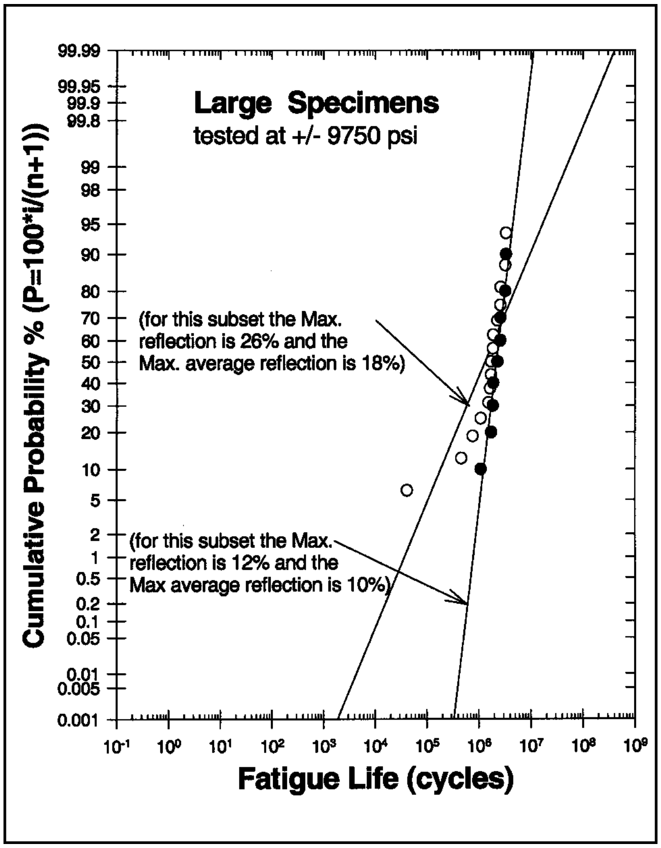

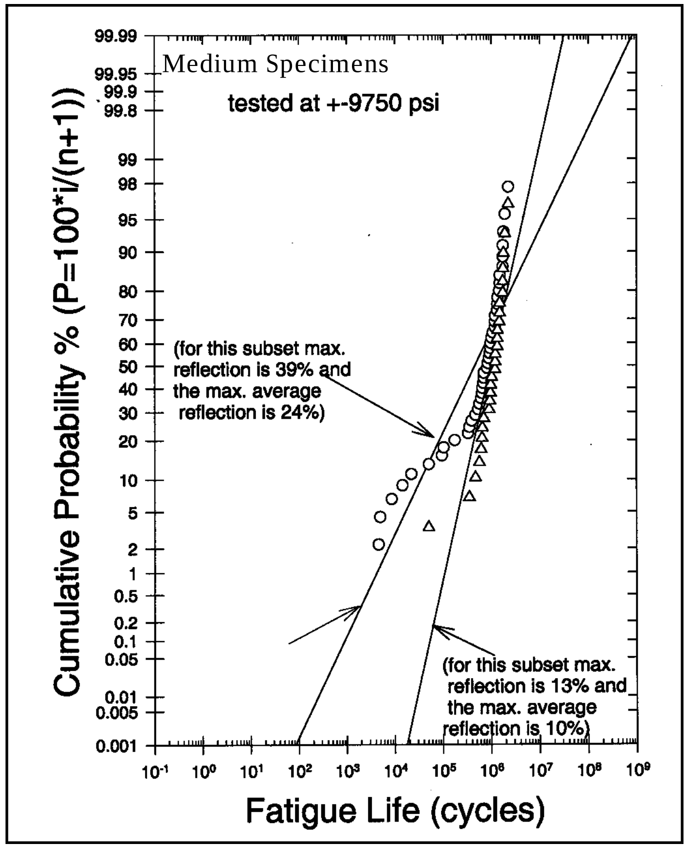

Fig. 10 — Cumulative probability for specimens tested at ±9750 lb/in.^{2} (±67 MPa).

Fig. 11 — Cumulative probability for specimens tested at ±9750 lb/in.^{2} (±67MPa).

sonably good job of explaining most, but not all, of the variation in the fatigue life.

All but three of the data points in Figs. 6–8 were within about two orders of magnitude of their expected value. There was only one data point in all those shown in Figs. 6–8 that was off the model line by as much as about three orders of magnitude. This was the point in Fig. 8 with an average reflection of 8%, but a life of only 200 cycles. The fracture surface of this specimen is shown in Fig. 3. While the average of all transducers was only 8%, there was a large local unbrazed region (with an individual channel reflection of 19%) that caused the fatigue life to be much less than what was expected. It is thus necessary to consider the reflections of each transducer (which defines the LOB at a specific area) as well as the average of all of the transducers. Hence, quality limits were placed on the maximum allowable reflection of an individual transducer, as well as on the average of all of the transducers. This reflects the fact that lack of brazing distribution is important, as well as the average LOB.

Figures 6–8 show that while the model explains much of the systematic variation of fatigue life, there can be variations of 1–2 orders of magnitude in fatigue life with respect to the model's trend line. Thus, even with knowledge of the LOB for each joint, there can still be a considerable uncertainty as to the fatigue life of an individual joint. It is thus necessary to consider the statistical variation of the fatigue lives in order to determine the predicted fatigue behavior. This is done in the cumulative probability plots of Figs. 9–12.

Figures 9–12 show the cumulative probability curves (discussed in the appendix) are altered by considering data sets that use only the results obtained from specimens exhibiting a restricted range of reflections (limited LOB allowed). The effect of restricting the allowable reflections is to decrease the standard deviation of the data set. This causes the curves to be steeper. The average fatigue life is not necessarily increased by an appreciable amount, so the probability plots can cross. The behavior when an extrapolation is made to a low probability of failure is critical, and here, the more restricted the data set, the longer the fatigue life. For instance, let us consider the data of Fig. 10. If a cumulative probability of failure of only 0.001% is desired, then, if a criteria of an average reflection of 18% and maximum reflection of 26% is utilized, the fatigue life is predicted to be about 2000 cycles. This means that at 2000 cycles, it would be expected that 0.001% of the specimens or parts experiencing ±9750 lb/in.^{2} (±67MPa) would have failed. If a criteria of an average reflection of 10% and maximum reflection of 12% are utilized, then it would be expected it would require more than 300,000 cycles for 0.001% of the samples or parts to fail. A similar analysis can be made for each of the stress ranges utilized, for the different criteria utilized and for the different cumulative probabilities for failure.

The data of Figs. 9–12 are not all log normal, *i.e.*, there are considerable deviations from linear behavior in many of the figures. This difficulty can be overcome, in part at least, by considering a Weibull distribution function. This will be done shortly, but first we shall consider the behavior at the design stress of ±5500 lb/in.^{2} (±38 MPa). To do this, it is necessary to translate all the data to ±5500 lb/in.^{2}, which is done in Fig. 13. This translation was accomplished by using the data of Fig. 5, which was used to develop Equation 1. The fatigue life of each data point was corrected using

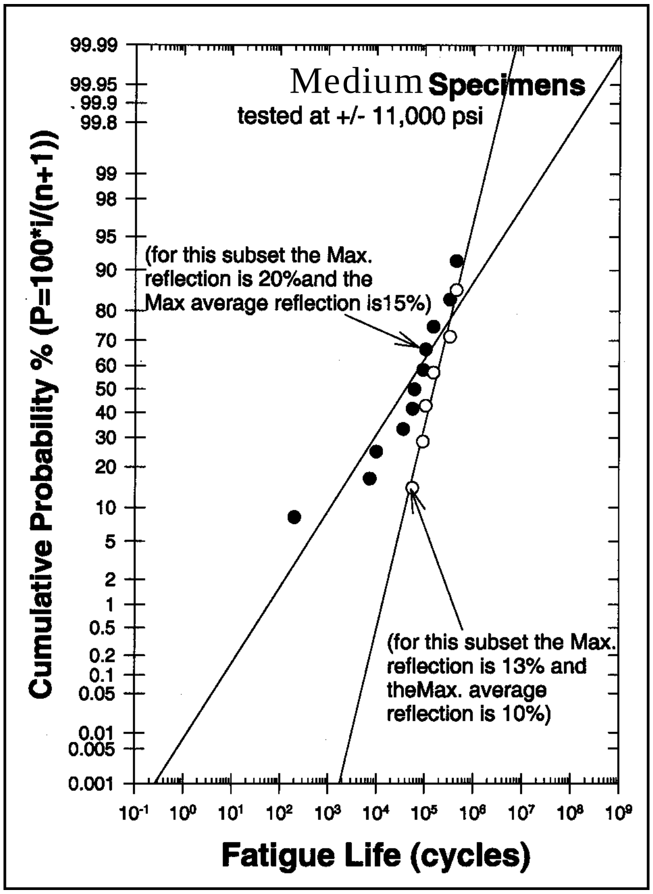

Fig. 12 — Cumulative probability for specimens tested at ±11,000 lb/in.^{2} (±76 MPa).

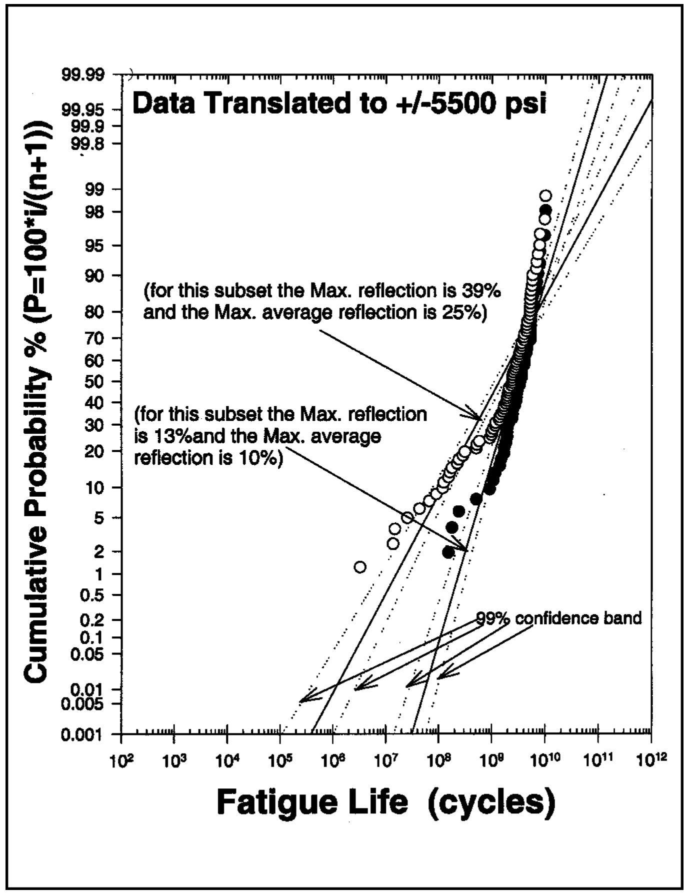

Fig. 13 — Cumulative probability for extrapolated to ±5500 lb/in.^{2} (±38 MPa).

Equation 1. This was accomplished by multiplying the fatigue life of each point by the ratio of the fatigue life at 5500 lb/in.^{2} as predicted by Equation 1, by the value Equation 1 predicts for the stress of that test. For instance, the fatigue life of each test run at ±8500 lb/in.^{2} (±59 MPa) is corrected by 3 x 10^9/6.74 x 10^6 = 445. The tests run at the higher stresses are corrected by larger amounts. Inherent in this approach is the assumption the distribution is independent of the stress range (*i.e.*, the standard deviation, or Weibull shape parameter, is independent of the stress level used in the test group). While not a bad assumption for this data, this is not always true (Ref. 9), as the standard deviation tends to increase as the stress level decreases. When this is the case, a maximum likelihood approach should be used (Ref. 9).

Figure 13 shows the data correlated for a maximum average reflection of 25% and maximum reflection of 39%, and for a maximum average reflection of 10% and a maximum reflection of 13%. These criteria encompass all the criteria used for the data that makes up this figure. The 99% confidence bands are also shown. The data of Fig. 13 does not appear to be very log normal, *i.e.*, the data deviates considerably from a straight line. This deviation does not correlate with the individual data sets. This is to say, the data for each set are interspersed and do not layer as individual groups. The lack of normal behavior has prompted the use of the Weibull parameter to correlate this data. This is done in Figs. 14 and 15.

The data of Fig. 14 are fit reasonably well by a straight line when the Weibull parameter function is plotted vs. the log of the fatigue life. The Weibull slopes of 0.70 and 1.24 illustrate this data does not conform to a log normal distribution (the distribution is very close to being normal when the shape factor is 3.57). Note, as is shown in the appendix, the Weibull slope is determined from a natural Ln plot, while the data has been shown on a common log plot so that the fatigue lives can be read directly. The resulting curve fit slope must be corrected by 2.3, or the curve fitting should be done on a Ln plot.

Figure 14 shows when a criteria of a maximum average reflection of 10% and a maximum reflection of any channel of 13% is used, then the mean life at W = –12.72 is greater than 1.5 x 10^5 cycles. (This W value corresponds to a probability of failure of 3 x 10^{-6} and is used to define "six sigma" reliability.) At this W value, there is a 99% probability of having a fatigue life of greater than 6.5 x 10^4 cycles (based on the lower limit of the 99% probability curve instead of the mean curve). This compares to a design life of 10^4 cycles. It is clear, therefore, that even if this very high degree of reliability is desired, the inspection criteria can be set to allow reflections of somewhat greater than an average of 10% and maximum of 13%, but an inspection should not allow a maximum average reflection of 26%, or maximum reflection of 39%. Graphs of the sort shown in Fig. 14 can be used to trade-off the reliability vs. the acceptance criteria.

While the use of the Weibull, parameter, W (discussed in the appendix), allows standard graphing packages to be used, it is not the most accurate approach. A better approach is to use a program that can calculate a Weibull distribution function directly, as is shown in Fig. 15. This figure uses the same criteria of a maximum average reflection of 10% and a maximum reflection, in any channel, of 13%, as was used in Fig. 14. With this inspection criteria, the mean curve reaches a 3 x 10^{-4} probability of failure at about 3 x 10^5 cycles and the lower limit of the 99% confidence band at about 2 x 10^4 cycles. This is similar to, but not exactly the same as the result shown in Fig. 14. The Weibull slope is greater (1.347 vs. 1.240), but the 99% confidence band is somewhat wider. (These differences are due to the differences in how the Weibull statistics are employed. The approach of Fig. 15 is preferred.) The design criterion is met, even at the lower limit of the 99% confidence band, so the calculation could be re-done using joints with greater average and maximum reflections. This can be done until the design limit is just met, thus allowing the greatest number of acceptable joints, consistent with the design criterion of a 10,000 cycle fatigue life.

Conclusions

An ultrasonic inspection was used to characterize the braze coverage percentage of induction-brazed Cu joints. A simple model relating the average reflection of several transducers to this coverage, was used to describe the quality of the joints. It was found the average percent of reflection could be related to the fatigue life through a simple, net-section stress model. The average percent of reflection was equated to the LOB percentage. As the LOB increases, the load-bearing area decreases, increasing the stress and decreasing the fatigue life. An S-N curve was used to relate the stress to the fatigue life. This simple model explained the general trend of the decrease in fatigue life with LOB, but there was still a large distribution in the measured fatigue lives. The UT measurements were, therefore, used with a statistical analysis of the data in order to set inspection criteria and to guarantee the desired design life could be met.

The fatigue lives were treated statistically, using cumulative log normal and Weibull distributions. The data was filtered using the results of the ultrasonic inspection. Quality criteria, based on the maximum allowable average ultrasonic reflection and maximum reflection for any individual transducer, were developed. Ultrasonic inspection of every joint allowed the elimination of joints whose average reflection was greater than 10% or a reflection measured by any single transducer was greater than 13%. This reduced the scatter in the fatigue lives (*i.e.*, the Weibull shape parameter was increased). (The degree of increase depended upon the strictness of the reflection criteria that was used.)

It is important to note that to achieve a desired fatigue life of 10^4 cycles with the desired reliability (99% probability of less than three failures per million joints), the mean fatigue life had to be on the order of 10^9 cycles. This points up the need to over-design brazed joints so the mean fatigue life is many, many orders of magnitude greater than the design life.

Acknowledgments

The author would like to acknowledge the assistance of Mike

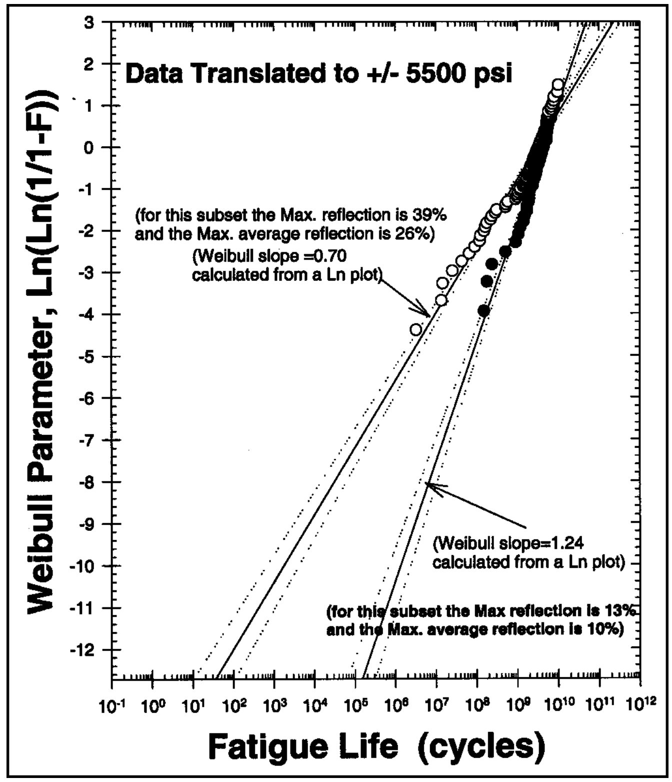

Fig. 14 — Data translated to ±5500 lb/in.² (±38 MPa) as correlated by the Weibull parameter, W.

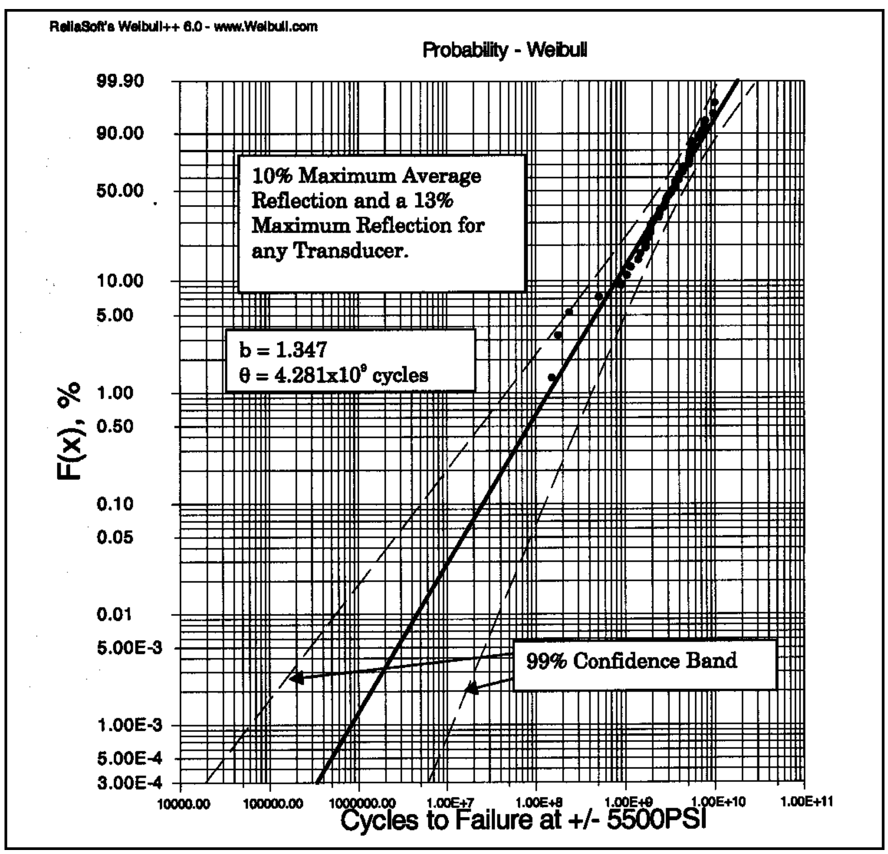

Fig. 15 — Weibull probability plots of data translated to ±5500 lb/in.² (±38 MPa), utilizing a 10% max. average reflection and 13% max. reflection criteria. (See the Appendix for a discussion of F(x), b and θ.)

Gilhooly, who performed all of the fatigue tests discussed here; Tony Barbuto, who performed the optical metallography; and Craig Robertson, who did the SEM work. The author would also like to acknowledge very fruitful discussions with Marcus Harrington, Jim Hopeck, Steve Hayashi and Jeff Stein.

References

1. Lee, C-K, Chin, B. A., Zinkle, S. J. and Wilcox, R. C. 1993. Mechanical properties of induction brazed Glidcop Al-15. *ASTM STP 1175*. ASTM, pp. 1026–1040.

2. Hatori, S., and Okada, T. Fatigue strength of silver filler brazed joints in nickel-copper alloys. *J. of Materials Science, Japan* V40(457), pp. 1330–1335 (in Japanese).

3. Dieter, G. E. 1983. Engineering statistics, Chapter 11. *Engineering Design, A Materials and Processes Approach*. New York, N.Y.: McGraw-Hill Book Co.

4. Weibull, W. 1961. *Fatigue Testing and Analysis of Results*. Oxford, N.Y.:Pergamon Press.

5. Weibull, W. 1939. A statistical theory of strength of materials, *Proc. Roy. Acad. Eng. Sci.*, No 15.

6. Weibull, W. A. 1951. Statistical distribution function of wide applicability. *J. Appl. Mech.* V18, pp. 293–297.

7. ASTM Subcommittee VI of ASTM Committee E-9. 1962. The Weibull distribution function for fatigue life. *Materials Research and Standards*, pp. 405–411.

8. Trantina, G. G. 1991. Statistical fatigue failure analysis. *J. of Testing and Evaluation*, pp. 44–49.

9. Meaker, W., and Escobar, L. 1998. *Statistical Methods for Reliability Data*. New York, N.Y.:John Wiley & Sons, Inc., pp. 593–597.

10. Bannantine, J. A., Comer, J. J., and Handrock, J. L. 1990. *The Fundamentals of Metal Fatigue Analysis*. Upper Saddle River, N.J.: Prentice Hall.

Appendix

Statistical Evaluation of Fatigue Data

The reader is directed to Refs. 2–9 for a fuller description of the statistical analysis of fatigue data. The following is presented to aid readers of this paper, and is in no way a complete discussion of this large topic.

If a large number of fatigue tests are run under the same conditions, there will be a range of measured fatigue lives. Generally, the variation in these measured values is greater than that of other mechanical properties, such as the yield or tensile strength. The measured values of the fatigue life (or any other measured parameter) can be ordered and, for complete or singly censored data, each value given an order or rank number according to

$$P(i) = i/(n+1) \qquad \text{(A1)}$$

where i is the order number and n the total number of measurements being ordered. (This is not the only order equation that has been proposed, but it is the simplest one and the one used here.) For instance, if nine measurements were made (*i.e.*, n = 9) then P(1) would equal 0.1. This means that this point is in the first decile of the sample. P(2) = 0.2 and so on. If P(i) is plotted on normal probability paper vs. the fatigue life (creating a cumulative distribution plot) and the data lie along a straight line, then the distribution is normal. This is almost never the case for fatigue data. Rather, a linear fit is often obtained when P(i) is plotted on normal probability paper vs. the log (or Ln) of the fatigue life. A linear fit shows the distribution is log normal. A log normal distribution plot can be used to determine the fatigue life at any level of reliability. For instance, in our example, the fatigue life of our P(5) plotting position point represents the fatigue life for the sample cumulative percentage failed at 50%. If 100 times P(i) of Equation 1 is plotted, then one can read the fatigue life for any desired percentage of failed specimens. What is generally required is an estimate of a very small percentage failed, 1% or less, when less than 100 specimens were tested. This would require extrapolating the cumulative distribution plot to 1% or below, with the attendant uncertainties that this entails.

Mathematically (Ref. 4), the cumulative distribution function of a variable X, F(x), is given by

$$F(x) = \int_{-\infty}^{x} f(x)\,dx \qquad \text{(A2)}$$

where f(x) is the probability density function. An estimate of the cumulative distribution function may be defined as the number of all individuals having an $X \le x$ divided by the total number of individuals (Ref. 4). The probability density function for a normal distribution is defined as

$$f(x) = (1/(\sigma\sqrt{(2\pi)}))*\exp[-1/2*((x-\mu)/\sigma)^2] \qquad \text{(A3)}$$

where σ is the standard deviation of the distribution and μ is the mean of the distribution. For a normal distribution, f(x) vs. x gives the typical bell-shaped curve centered on μ with a width defined by σ. Unfortunately, the integration of Equation 3 does not have a closed form. However, standard statistical tables list common values of the cumulative normal distribution, and normal probability paper is scaled such that rank ordered, normally distributed data will plot as a straight line. For fatigue data, the distribution is often log normal, that is to say normal when the log of the fatigue life is used.

Another cumulative distribution function (in addition to the cumulative log normal distribution) that is a good model for fatigue data is the one developed by Weibull (Refs. 3–8), *i.e.*, as

$$F(x) = 1-\exp[-(x/\theta)^b] \quad \text{for } x>0 \qquad \text{(A4)}$$

where b is the Weibull modulus or shape factor and θ is the characteristic value. When x = θ, then Equation A4 reduces to 1–1/e, which is equal to 0.632. In other words, θ defines the characteristic value of the fatigue life where 63.2% of a Weibull distributed population would fail. The great power of a Weibull distribution function is that it can describe an infinite number of types of distributions, depending upon the value of b. When b equals 1, the Weibull distribution becomes an exponential distribution. When it is 2, it is a Rayleigh distribution, and when it is 3.57, it becomes very nearly a normal distribution. The shape factor and characteristic value can be determined by rank ordering the data and plotting P(i) for each point vs. the fatigue life on Weibull paper and fitting a straight line through the points. The slope of this line is an estimate of the shape factor b, and the characteristic value θ is the fatigue life corresponding to the 63.2nd percentile. Equation A4 can also be rewritten as

$$1/(1-F(x)) = \exp(x/\theta)^b \qquad \text{(A5)}$$

or

$$\ln[1/(1-F(x))] = (x/\theta)^b \qquad \text{(A6)}$$

or

$$W = \ln(\ln[1/(1-F(x))]) = b[\ln(x) - \ln(\theta)] \qquad \text{(A7)}$$

When evaluating Equation A7, the plotting position P(i) is used for F(x) and x is the fatigue life corresponding to the rank ordered number point i. This enables one to use regular, semilog graph paper (or a graphing program).

There is a also a three-parameter Weibull distribution function where the fatigue life is considered relative to a minimum value x_0. The formulation of the distribution law is unchanged except $(x-x_0)$ is considered rather than x. The simpler two parameter Weibull distribution function, described by Equation A7, was use, in the study presented here. While W can be calculated and used to determine the Weibull statistics, it is better to base any predictions on a fit to Equation A4, rather than fitting the W values. This can be accomplished with several commercial statistical programs. A fit to the W parameter minimizes the error in W, which has been determined using a double Ln function. When F(x) is used via the appropriate statistical program, the fit minimizes the error in F(x), which is the correct approach.